

# Non-linear Distance-based Semi-supervised Multi-class Gesture Recognition

Husam Al-Behadili<sup>1,2</sup>, Arne Grumpe<sup>2</sup> and Christian Wöhler<sup>2</sup>

<sup>1</sup>Electrical Engineering, University of Mustansiriyah, Al-Mustansiriyah, Box 46007, Baghdad, Iraq

<sup>2</sup>Image Analysis Group, TU Dortmund University, Otto-Hahn-Str. 4, D-44227, Dortmund, Germany

**Keywords:** Data Stream, Nearest Class Mean, Incremental Learning, Semi-supervised Learning, Kernel.

**Abstract:** The automatic recognition of gestures is important in a variety of applications, e.g. human-machine-interaction. Commonly, different individuals execute gestures in a slightly different manner and thus a fully labelled dataset is not available while unlabelled data may be acquired from an on-line stream. Consequently, gesture recognition systems should be able to be trained in a semi-supervised learning scenario. Additionally, real-time systems and large-scale data require a dimensionality reduction of the data to reduce the processing time. This is commonly achieved by linear subspace projections. Most of the gesture data sets, however, are non-linearly distributed. Hence, linear sub-space projection fails to separate the classes. We propose an extension to linear subspace projection by applying a non-linear transformation to a space of higher dimensional after the linear subspace projection. This mapping, however, is not explicitly evaluated but implicitly used by a kernel function. The kernel nearest class mean (KNCM) classifier is shown to handle the non-linearity as well as the semi-supervised learning scenario. The computational expense of the non-linear kernel function is compensated by the dimensionality reduction of the previous linear subspace projection. The method is applied to a gesture dataset comprised of 3D trajectories. The trajectories were acquired using the Kinect sensor. The results of the semi-supervised learning show high accuracies that approach the accuracy of a fully supervised scenario already for small dimensions of the subspace and small training sets. The accuracy of the semi-supervised KNCM exceeds the accuracy of the original nearest class mean classifier in all cases.

## 1 INTRODUCTION

The recognition of gestures has become an important element of human-machine interaction. Since the amount of available gesture data is small and does not cover all possible manners of performing a gesture, the classification system may benefit from semi-supervised learning to adapt to new users. A large amount of unlabelled gesture data may be available or acquired on-line. Semi-supervised learning, i.e. pre-training the classifier on a supervised dataset and updating the training set using the labels assigned by the classifier (Zhu and Goldberg, 2009), solves these problems in different applications of machine learning. However, the problems arising here are possibly non-linearly separable distributions of the data, high dimensionality, computational complexity of classifier retraining and potentially false labels assigned by the classifier that will effect the performance of the classifier after the next training cycle. Hence, it is desirable to design a system that may operate us-

ing low-dimensional subspace projections of the data while still being able to separate non-linearly separable data distributions with high accuracy to guarantee the success of the semi-supervised learning. This work focuses on the recognition of emblematic gestures which are performed in 3D space with one arm and acquired with a Kinect sensor.

### 1.1 Related Work

Metric learning is an important concept for both unsupervised and semi-supervised learning. Examples of metric learning are k-nearest neighbour (kNN) (Guillaumin et al., 2009; Cover and Hart, 1967; Boiman et al., 2008; Altman, 1992), prototype learning with adaptive distance metric (Schneider et al., 2009), Nearest Class Mean (NCM) (Webb, 2003), and Nearest Class Mean Multi-class Loistic Discrimination (NCMC) (Mensink et al., 2013a,b). A kNN classifier determines the distance between a sample to be classified and each training sample. The method proposed

by Schneider et al. (2009) provides a representation of the training set based on prototype vectors and assigns a sample to a class based on an appropriately chosen or learned distance metric. In the NCM method suggested by Webb (2003), the Mahalanobis distance between the query sample and the class-specific sample mean vectors measures the similarity between the query sample and the classes. The NCMC framework extends the NCM method applying an optimal projection that enforces the samples within the same class to have a smaller distance to its corresponding class mean than samples from other classes (Mensink et al., 2013a,b).

## 1.2 Contribution

The performance of the classifier in semi-supervised learning scenarios is very sensitive to the classifier accuracy in the previous classification process. Hence, we need to build a classifier that is robust against outliers, has high accuracy, and is quickly retrained in near constant time. The NCMC classifier proposed by Mensink et al. (2013a) uses a linear subspace projection approximating the covariance matrix to reduce the computational complexity of modern high-dimensional classification problems. Most gesture datasets, however, are not linearly separable. We extend the NCMC towards linearly unseparable datasets by applying the kernel trick to improve the performance of the NCMC in such environments and make it less sensitive to the dimensionality of the data. To avoid an increased runtime, the kernel function is applied after the linear subspace projection. The proposed algorithm shows an increased accuracy in both linear and non-linear system as well as a reduced time of processing in most cases.

## 2 FUNDAMENTALS

### 2.1 Non-linear Nearest Class Mean with Multiple Class Centroid (NCMC)

The nearest class mean classifier implemented by Mensink et al. (2013a) looks for the closest centroid  $\boldsymbol{\mu}_c$  of class  $c$  to assign the corresponding class label to the instance with feature vector  $\mathbf{x}$  of dimensionality  $D$ . If we have a new sample  $\mathbf{x}$ , the distance between this sample and the centroid  $\boldsymbol{\mu}_c$  of class  $c$  is  $d(\mathbf{x}, \boldsymbol{\mu}_c)$ . This new sample is labelled by  $\hat{c}$ , corresponding to the class with the minimum distance among the distances from  $N_{\text{classes}}$  classes to this sample:

$$\hat{c} = \underset{c \in \{1, \dots, N_{\text{classes}}\}}{\operatorname{argmin}} d(\mathbf{x}, \boldsymbol{\mu}_c). \quad (1)$$

The centroid of class  $c$  is the mean of the  $N_c$  instances  $\mathbf{x}_i$  of class  $c$ :

$$\boldsymbol{\mu}_c = \frac{1}{N_c} \sum_{i=1}^{N_c} \mathbf{x}_i. \quad (2)$$

The squared Mahalanobis distance specified by the covariance matrix  $\mathbf{M}$ , i.e.

$$d(\mathbf{x}, \boldsymbol{\mu}_c) = (\mathbf{x} - \boldsymbol{\mu}_c)^T \mathbf{M} (\mathbf{x} - \boldsymbol{\mu}_c), \quad (3)$$

was applied by Mensink et al. (2013a). Furthermore, it is assumed by Mensink et al. (2013a) that  $\mathbf{M} = \mathbf{W}^T \mathbf{W}$ , since  $\mathbf{M}$  is a positive semi-definite matrix. The matrix  $\mathbf{W} \in \mathbb{R}^{h \times D}$  is a low-rank metric and  $h \leq D$  is the effective dimension of the subspace projection. Consequently,

$$\begin{aligned} d(\mathbf{x}, \boldsymbol{\mu}_c) &= (\mathbf{x} - \boldsymbol{\mu}_c)^T \mathbf{W}^T \mathbf{W} (\mathbf{x} - \boldsymbol{\mu}_c) \\ &= \|\mathbf{W}\mathbf{x} - \mathbf{W}\boldsymbol{\mu}_c\|_2^2. \end{aligned} \quad (4)$$

The posterior of the class  $c$  given an instance  $\mathbf{x}$  is defined by Mensink et al. (2013a) as

$$p(c|\mathbf{x}) = \frac{\exp\left(-\frac{1}{2}d(\mathbf{x}, \boldsymbol{\mu}_c)\right)}{\sum_{\hat{c}=1}^{N_{\text{classes}}} \exp\left(-\frac{1}{2}d(\mathbf{x}, \boldsymbol{\mu}_{\hat{c}})\right)} \quad (5)$$

assuming uniformly distributed classes and a normally distributed likelihood, i.e.  $p(\mathbf{x}|c) = \mathcal{N}(\boldsymbol{\mu}_c, \mathbf{W}^T \mathbf{W})$ . The covariance  $\mathbf{W}^T \mathbf{W}$  is shared across all classes. The log-posterior of the correct prediction is maximized using a stochastic gradient descent to obtain the optimal projection matrix  $\mathbf{W}$  (Mensink et al., 2013a).

For non-linear spaces, the single centroid of each class is replaced by Mensink et al. (2013a) by multiple prototypes, which are obtained using the  $k$ -means algorithm. The query samples are then assigned to the class of the nearest centroid. Assuming a mixture of normal distributions centred at the  $N_{\text{centroids}}$  centroids  $\mathbf{m}_{c,j}$ ,  $j \in \{1, \dots, N_{\text{centroids}}\}$  for each class  $c$ , the posterior probability of class  $c$  is defined by Mensink et al. (2013a) as

$$p(c|\mathbf{x}) = \sum_{j=1}^{N_{\text{centroids}}} p(\mathbf{m}_{c,j}|\mathbf{x}), \quad \text{with} \quad (6)$$

$$p(\mathbf{m}_{c,j}|\mathbf{x}) = \frac{\exp\left(-\frac{1}{2}d(\mathbf{x}, \mathbf{m}_{c,j})\right)}{\sum_{c=1}^{N_{\text{classes}}} \sum_{j=1}^{N_{\text{centroids}}} \exp\left(-\frac{1}{2}d(\mathbf{x}, \mathbf{m}_{c,j})\right)}. \quad (7)$$

### 2.2 Kernel based Metrics

Kernels are proposed to solve non-linear separation problems in different types of machine learning algorithms. As described in detail by Theodoridis et al.

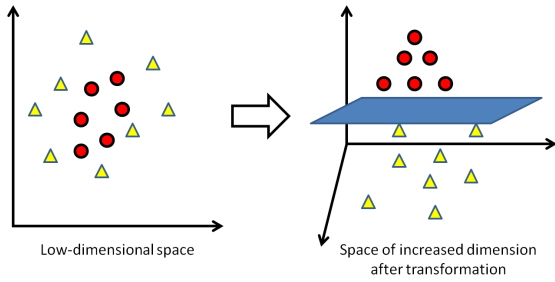


Figure 1: Kernel trick. By transforming the original space (left) into a space of increased dimension (right) the two classes circle and square become linearly separable. Adapted from Elmezain et al. (2009).

(2010), the transformation  $\Phi : \mathbb{R}^D \times \mathbb{R} \rightarrow \mathbb{R}^{\mathcal{H}}$  is a generally non-linear transformation of the feature space  $\mathbb{R}^D$  to a space  $\mathbb{R}^{\mathcal{H}}$  of increased dimension  $\mathcal{H}$ . Due to the transformation  $\Phi$ , a linear separation, i.e. a separating hyperplane, in  $\mathbb{R}^{\mathcal{H}}$  becomes a non-linear separating function when projected back onto the original feature space. Consequently, the classes may become linearly separable after the transformation into the space of increased dimension. An example is shown in Fig. 1.

Commonly, it is sufficient to compute inner products in the higher dimensional space, e.g. computing the Euclidean distance of samples from the separating hyperplane. The so-called “kernel Trick” utilizes this fact. As shown by Theodoridis et al. (2010), if the mapping of the vectors  $\mathbf{x}$  and  $\hat{\mathbf{x}}$  satisfies Mercer’s theorem it is not required to evaluate or know the mapping  $\Phi$ , and the inner product may be replaced by the kernel function

$$K(\mathbf{x}, \hat{\mathbf{x}}) = \langle \Phi(\mathbf{x}), \Phi(\hat{\mathbf{x}}) \rangle_{\mathcal{H}} = \Phi(\mathbf{x})^T \Phi(\hat{\mathbf{x}}). \quad (8)$$

Consequently, it is possible to evaluate the inner product in the high dimensional space by applying a possibly non-linear kernel function  $K(\mathbf{x}, \hat{\mathbf{x}})$  to the representations  $\mathbf{x}$  and  $\hat{\mathbf{x}}$  in the original space. Examples of common kernel functions are polynomial kernels or Gaussian kernels (Theodoridis et al., 2010). In this work, the kernel function is a radial basis function (RBF) of Gaussian shape given by

$$K_{\text{RBF}}(\mathbf{x}, \hat{\mathbf{x}}) = \exp\left(-\frac{\|\mathbf{x} - \hat{\mathbf{x}}\|_2^2}{(2\sigma^2)}\right), \quad (9)$$

where  $\sigma$  denotes the predefined width of the kernel function. The Gaussian RBF kernel is shift-invariant. Consequently, the similarity metric learned using RBF kernels will be coordinate-independent (Kung, 2014).

### 3 PROPOSED KERNEL NCM (KNCM)

This work extends the work of Al-Behadili et al. (2015), who proposed a kernel-based distance metric. We extend this idea towards semi-supervised learning of non-linearly separable classes using a low-dimensional kernel-based data representation. Recalling the distance proposed by Mensink et al. (2013a)  $d(\mathbf{x}, \boldsymbol{\mu}_c) = \|\mathbf{W}\mathbf{x} - \mathbf{W}\boldsymbol{\mu}_c\|_2^2$  and setting  $\tilde{\mathbf{x}} = \mathbf{W}\mathbf{x}$  and  $\tilde{\boldsymbol{\mu}}_c = \mathbf{W}\boldsymbol{\mu}_c$ , the distance becomes

$$d(\mathbf{x}, \boldsymbol{\mu}_c) = \|\tilde{\mathbf{x}} - \tilde{\boldsymbol{\mu}}_c\|_2^2 = \tilde{\mathbf{x}}^T \tilde{\mathbf{x}} - \tilde{\mathbf{x}}^T \tilde{\boldsymbol{\mu}}_c - \tilde{\boldsymbol{\mu}}_c^T \tilde{\mathbf{x}} + \tilde{\boldsymbol{\mu}}_c^T \tilde{\boldsymbol{\mu}}_c. \quad (10)$$

Applying the transformation to a higher-dimensional space to  $\tilde{\mathbf{x}}$  and  $\tilde{\boldsymbol{\mu}}_c$ , respectively, yields the kernel based distance

$$d_{\text{kernel}}(\tilde{\mathbf{x}}, \tilde{\boldsymbol{\mu}}_c) = K(\tilde{\mathbf{x}}, \tilde{\mathbf{x}}) - K(\tilde{\mathbf{x}}, \tilde{\boldsymbol{\mu}}_c) - K(\tilde{\boldsymbol{\mu}}_c, \tilde{\mathbf{x}}) + K(\tilde{\boldsymbol{\mu}}_c, \tilde{\boldsymbol{\mu}}_c), \quad (11)$$

which, in case of a Gaussian RBF, is given by

$$d_{\text{kernel}}(\mathbf{x}, \boldsymbol{\mu}_c) = 2 - 2 \exp\left(-\frac{\|\mathbf{W}\mathbf{x} - \mathbf{W}\boldsymbol{\mu}_c\|_2^2}{2\sigma^2}\right). \quad (12)$$

Adopting the approach of Mensink et al. (2013a) we obtain the posterior probability

$$p(c|\mathbf{x}) = \frac{\exp(-\frac{1}{2}d_{\text{kernel}}(\mathbf{x}, \boldsymbol{\mu}_c))}{\sum_{\tilde{c}=1}^{N_{\text{classes}}} \exp(-\frac{1}{2}d_{\text{kernel}}(\mathbf{x}, \boldsymbol{\mu}_{\tilde{c}}))} \quad (13)$$

and compute the matrix  $\mathbf{W}$  by maximizing the log-posterior of the correct prediction using gradient ascent.

### 4 DATASET

Since KNCM is proposed to work with non-linear systems without losing the key features of NCMC, i.e. the accuracy and the short processing time, we apply it to a non-linearly separable gesture dataset. We will evaluate and compare the recognition performance of the KNCM approach with that of the the NCMC method.

A Kinect sensor has been used by Fothergill et al. (2012) to acquire a database of gestures which are mainly performed with both hands simultaneously. A database of emblematic gestures performed with a single forearm and hand has been published by Richarz and Fink (2011), where the 3D trajectories were inferred from stereo image data. A dataset

of single-arm emblematic gestures acquired with a Kinect sensor is described by Al-Behadili et al. (2014)<sup>1</sup>. We use the dataset of Al-Behadili et al. (2014), but since each gesture is repeated three times in the published version, we performed a subdivision of the dataset into single repetitions, resulting in 2878 gestures altogether. The first six features are adopted from Al-Behadili et al. (2014): three features for the  $x$ ,  $y$  and  $z$  coordinates of the mean vector, and three features for the extension along the  $x$ ,  $y$  and  $z$  axis. The motion direction is transformed into the seventh feature as follows:

- A principal component analysis of the dataset is performed. A 3D trajectory is considered a two-axes gesture if the projection on the eigenvector belonging to the second-largest eigenvalue is larger than 60% of the projection on the eigenvector belonging to the largest eigenvalue. In this case, the first two principal components are kept for the subsequent analysis. Otherwise, only the first principal component is kept as the gesture then is a one-axis gesture.
- The signs of the selected principal components are computed for each coordinate.
- A value of 1 (2) is assigned if more than 80% of the coordinates are positive (negative). In the case of no predominant direction, a value of 3 is assigned. Principal components not selected by the described procedure are assigned a value of 0.
- The assigned direction values are concatenated in the order of the principal components, forming a base-4 number which is then transformed to a decimal number denoting the direction information.

The total length of the normalized gesture is taken as the last feature. We found this compact set of features to be a favourable choice after having performed many experiments with more extensive feature sets proposed by e.g. Bhuyan et al. (2008) and Yoon et al. (2001) including position, speed, direction, orientation, curvature, chain code etc.

## 5 EXPERIMENTS AND RESULTS

### 5.1 Experimental Setup

Since falsely assigned labels have a strong effect on the performance of a semi-supervised learning algorithm, we introduce a confidence threshold and reject possible outliers, i.e. samples exceeding a dis-

tance threshold. The labels of samples that do not exceed the threshold are added to the training dataset of the classifier. The same approach is applied to the KNCM and the NCMC classifiers, respectively. We used the code of NCMC<sup>2</sup> as published by Mensink et al. (2013a).

The threshold is based on an independent validation dataset. Consequently, the full dataset is subdivided into four parts: a labelled initial training set, a labelled validation set, an unlabelled learning set and a labelled test set. At the beginning of the experiment, the classifiers are adapted to the initial training set and the confidence threshold is computed based on the validation set. The learning set is further subdivided into so-called “buckets” that represent a stream of data. The buckets are presented to the classifiers one by one. The classifiers then assign labels to the samples contained in the bucket, respectively, and add the samples that do not exceed the training threshold with the assigned labels to the training data. Then the classifiers are adapted to the extended training set, and a new confidence threshold is computed. This process is repeated until the last bucket has been presented to the classifiers. After each training process of the classifiers, we evaluate the accuracy of the classifiers based on the test set. In addition to the accuracy, we track the computation time required by each training and prediction stage and the training set size. Additionally, we train a second version of each classifier with the correct labels to evaluate the performance of a fully supervised learning scenario in each step.

The semi-supervised learning experiment is repeated for three different sizes of the initial training set: 1%, 5% and 10% of the total dataset. In all experiments, the test and the validation set comprise 20% and 15% of the total dataset, respectively. The remainder is the unlabelled learning set, which is subdivided into buckets of 100 samples each. The sets are formed using a class-wise random partition, i.e. 1% of the training set corresponds to 1% of the samples from each class, respectively. Since each of the nine gestures in the dataset is represented by a different amount of samples, the amount of samples in the initial training set may be as low as two samples in the case of class nine and an initial training set comprising 1% of the total data. Each experiment is repeated for four different dimensions of the subspace  $h = \{2, 4, 6, 8\}$ , respectively, resulting in twelve different experiments. Due to the random partition of the data, the results of the experiments may depend on how the initial training set has been selected. To estimate the expected outcome of the experiment, each experiment is repeated 100 times with a differ-

<sup>1</sup>The complete dataset is available at <http://www.bv.e-technik.tu-dortmund.de>

<sup>2</sup><https://staff.fnwi.uva.nl/t.e.j.mensink/code.php>

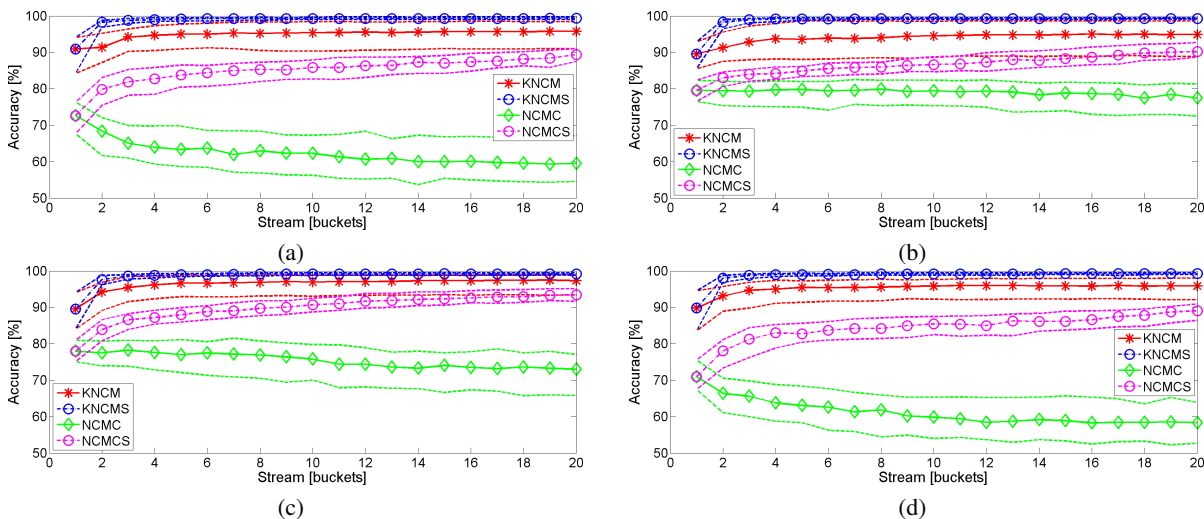


Figure 2: Median prediction accuracy of the classifiers for an initial training set comprising 1% of the total data. KNCMS and NCMCS denote the supervised version of the KNKM and NCMC, respectively. The dashed lines correspond to the 25% and 75% quantiles and represent the spread over 100 repetitions. (a)  $h = 2$ . (b)  $h = 4$ . (c)  $h = 6$ . (d)  $h = 8$ .

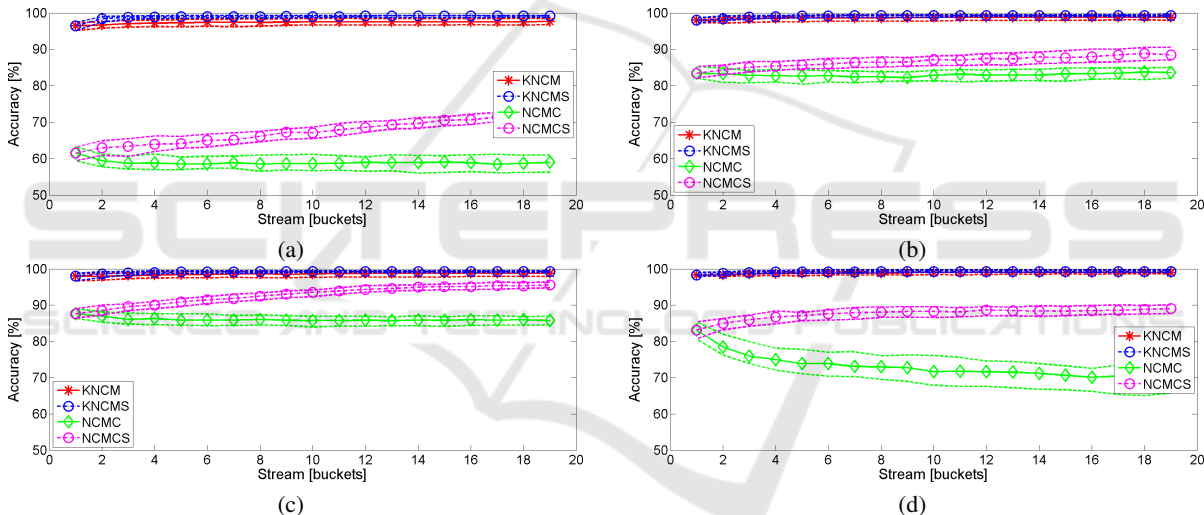


Figure 3: Median prediction accuracy of the classifiers for 5% of the total data used as initial training set. KNCMS and NCMCS denote the supervised version of the KNKM and NCMC, respectively. The dashed lines correspond to the 25% and 75% quantiles and represent the spread over the 100 repetitions. (a)  $h = 2$ . (b)  $h = 4$ . (c)  $h = 6$ . (d)  $h = 8$ .

ent random permutation. Both classifiers use the same random permutation for each experiment during these 100 repetitions.

The NCMC requires the specification of the number of centroids per class  $N_{centroids}$ . There is, however, a function within the utilised code package published by Mensink et al. (2013a) that computes the optimal number of centroids per class. We apply this code to specify the best  $N_{centroids}$  for each projection matrix dimension. The resulting values were  $N_{centroids} = 2$  for the four dimensions of the subspace, respectively. In case of  $N_{centroids} > N_c$ , i.e. the number of class  $c$  samples in the initial training is smaller than the num-

ber of centroids, we start by setting  $N_{centroids} > N_c$  and then gradually increase  $N_{centroids}$  until it equals the optimal value.

## 5.2 Results and Performances Study

Figs. 2–4 show the prediction accuracy of KNKM and NCMC. Notably, the first bucket corresponds to the initial training set. The remaining results thus may be directly compared to the result obtained by using the initial training set. For large training sets (see Fig. 4), the accuracy of the KNKM equals the accuracy of the supervised version. The high initial accuracy

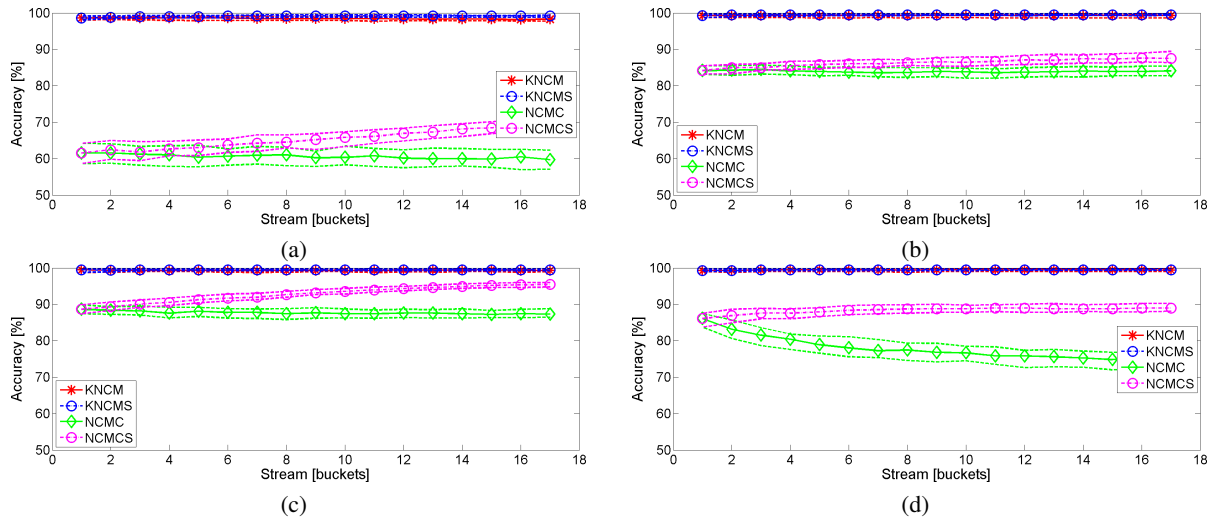


Figure 4: Median prediction accuracy of the classifiers for 10% of the total data used as initial training set. KNCMS and NCMCS denote the supervised version of the KNKM and NCMC, respectively. The dashed lines correspond to the 25% and 75% quantiles and represent the spread over the 100 repetitions. (a)  $h = 2$ . (b)  $h = 4$ . (c)  $h = 6$ . (d)  $h = 8$ .

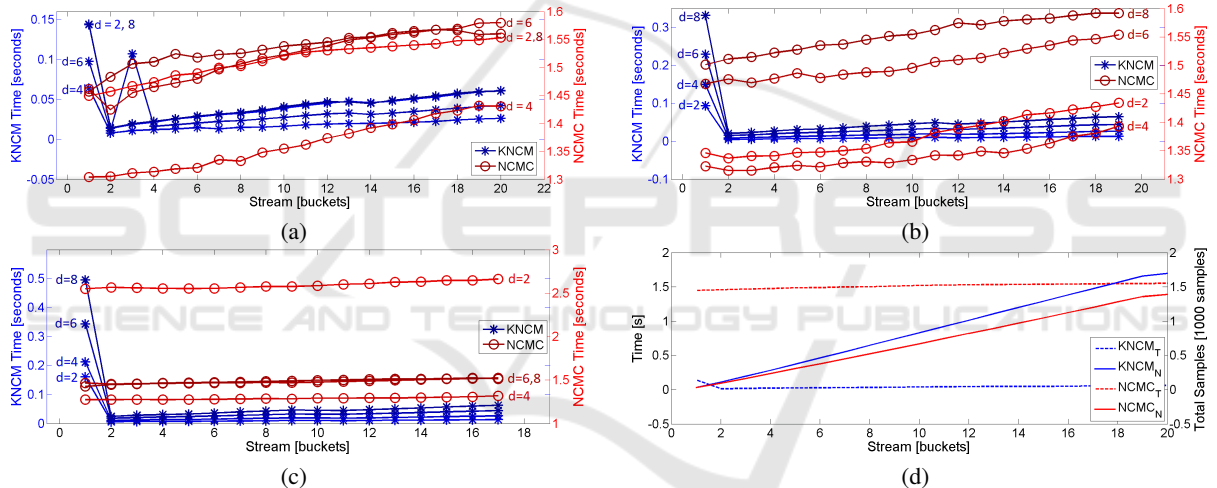


Figure 5: Time consumed by the classifiers. (a) Initial training set: 1% of total data. (b) Initial training set: 5% of total data. (c) Initial training set: 10% of total data. (d) Runtime (KNKM<sub>T</sub> and NCMC<sub>T</sub>) and samples in the training set (KNKM<sub>N</sub> and NCMC<sub>N</sub>) for the KNKM and the NCMC, respectively. The initial training set size is 1% of the total data, and the dimensionality is  $h = 2$ .

is kept throughout the learning process. If the size of the training set is reduced (see Fig. 2–3) the accuracy of the semi-supervised KNKM does not reach the optimal value of the fully supervised KNKM. It, however, increases strongly over the first few buckets and approaches the fully supervised KNKM. The difference between the semi-supervised KNKM and the fully supervised KNKM increases with decreasing dimensions of the projection subspace. However, the effect of the subspace dimension on the KNKM accuracy is rather subtle and thus it is possible to use subspace projections of very low dimension.

The accuracy of the NCMC, in contrast, shows a

larger difference to its fully supervised counterpart if the number of presented buckets increases. While the fully supervised NCMC shows an increasing accuracy in the course of the learning experiment, the accuracy of the semi-supervised NCMC seems constant in the best case and exhibits a strong decrease in some experiments. Both the semi-supervised NCMC and the fully supervised NCMC do not reach the accuracy of the KNKM in all experiments. The decreasing accuracy of the NCMC suggests that the NCMC adds false labels to the training set. This may be due to the low initial prediction accuracy. The effect is less noticeable if the size of the training set increases. Further-

more, this effect seems to be strong for both the full dimension of the data set and a very small subspace dimension. The former may be related to the estimation of many parameters while the latter may be due to insufficient subspace dimension that does not allow for a separation of the classes.

In addition to the gain in prediction accuracy, the runtime of the KNCM is considerably lower than the runtime of the NCMC, as shown in Fig. 5. The decreasing accuracy of the NCMC suggests that the NCMC method results in the addition of more false labels to the training set, possibly leading to a larger total number of samples. However, the opposite is true. Fig. 5(d) shows the median runtime and the median of the training set size for an initial training set comprising 1% of the total data and a dimensionality of  $h = 2$ . This exemplary semi-supervised learning progress is similar to the other experiments. Fig. 5(d) clearly shows that the runtime is independent of the training set size.

## 6 CONCLUSION

The proposed KNCM shows an increased accuracy and a lower runtime in comparison to the original NCMC. The high accuracy is maintained for extremely small dimensional subspace projections. Furthermore, the KNCM and its ability to reject outliers has been demonstrated in a semi-supervised learning scenario of gestures. The semi-supervised KNCM achieves accuracies that are comparable to a fully supervised learning scenario. Since the proposed algorithm is not limited to gesture data, it is expected to be applicable to any semi-supervised learning scenario.

## REFERENCES

- Al-Behadili, H., Wöhler, C., and Grumpe, A. (2014). Semi-supervised learning of emblematic gestures. *AT-AUTOMATISIERUNGSTECHNIK*, 62(10):732–739.
- Al-Behadili, H., Wöhler, C., and Grumpe, A. (2015). Non-Linear Distance Based Large Scale Data Classifications. In *3<sup>rd</sup> International conference on image Information Processing (ICIIP)*, page In Press. IEEE.
- Altman, N. S. (1992). An introduction to kernel and nearest-neighbor nonparametric regression. *The American Statistician*, 46(3):175–185.
- Bhuyan, M., Bora, P., and Ghosh, D. (2008). Trajectory guided recognition of hand gestures having only global motions. *International Journal of Computer Science, Fall*.
- Boiman, O., Shechtman, E., and Irani, M. (2008). In defense of nearest-neighbor based image classification. In *Computer Vision and Pattern Recognition, 2008. CVPR 2008. IEEE Conference on*, pages 1–8. IEEE.
- Cover, T. and Hart, P. (1967). Nearest neighbor pattern classification. *Information Theory, IEEE Transactions on*, 13(1):21–27.
- Elmezain, M., Al-Hamadi, A., Rashid, O., and Michaelis, B. (2009). Posture and Gesture Recognition for Human-Computer Interaction. In Jayanthakumaran, K., editor, *Advanced Technologies*, pages 415–440. InTech, Rijeka, Croatia.
- Fothergill, S., Mentis, H., Kohli, P., and Nowozin, S. (2012). Instructing people for training gestural interactive systems. In *Proceedings of the SIGCHI Conference on Human Factors in Computing Systems*, pages 1737–1746. ACM.
- Guillaumin, M., Mensink, T., Verbeek, J., and Schmid, C. (2009). Tagprop: Discriminative metric learning in nearest neighbor models for image auto-annotation. In *Computer Vision, 2009 IEEE 12th International Conference on*, pages 309–316. IEEE.
- Kung, S. Y. (2014). *Kernel Methods and Machine Learning*. Cambridge University Press.
- Mensink, T., Verbeek, J., Perronnin, F., and Csurka, G. (2013a). Distance-based image classification: Generalizing to new classes at near-zero cost. *IEEE Transactions on Pattern Analysis and Machine Intelligence*, 35(11):2624–2637.
- Mensink, T., Verbeek, J., Perronnin, F., and Csurka, G. (2013b). Large scale metric learning for distance-based image classification on open ended data sets. In *Advanced Topics in Computer Vision*, pages 243–276. Springer.
- Richarz, J. and Fink, G. A. (2011). Visual recognition of 3d emblematic gestures in an hmm framework. *Journal of Ambient Intelligence and Smart Environments*, 3(3):193–211.
- Schneider, P., Biehl, M., and Hammer, B. (2009). Adaptive relevance matrices in learning vector quantization. *Neural Computation*, 21(12):3532–3561.
- Theodoridis, S., Pikrakis, A., Koutroumbas, K., and Cavouras, D. (2010). *Introduction to Pattern Recognition: A Matlab Approach*. Academic Press.
- Webb, A. R. (2003). *Statistical pattern recognition*. John Wiley & Sons.
- Yoon, H.-S., Soh, J., Bae, Y. J., and Yang, H. S. (2001). Hand gesture recognition using combined features of location, angle and velocity. *Pattern recognition*, 34(7):1491–1501.
- Zhu, X. and Goldberg, A. B. (2009). *Introduction to Semi-supervised Learning. Synthesis lectures on artificial intelligence and machine learning*. Morgan & Claypool Publishers.